CLM-R81

United Kingdom Atomic Energy Authority

RESEARCH GROUP

Report

THE CALCULATION OF PLASMA ELECTRON TEMPERATURE FROM ABSORPTION MEASUREMENTS OF CONTINUUM X-RADIATION FROM A PLASMA

J. H. ADLAM
I. C. TAYLOR

Culham Laboratory
Abingdon Berkshire

1968

Available from H. M. Stationery Office
THREE SHILLINGS NET

U.D.C.
533.9.082.5
533.933.12

UNCLASSIFIED
(Approved for Sale)

CLM - R 81

THE CALCULATION OF PLASMA ELECTRON TEMPERATURE FROM ABSORPTION MEASUREMENTS OF CONTINUUM X-RADIATION FROM A PLASMA

by

J.H. ADLAM
I.C. TAYLOR

A B S T R A C T

Two cases of continuum X-radiation, (1) from the volume of a plasma, and (2) from a target placed in a plasma, are considered. The ratio by which the X-ray intensity is reduced on passing through an absorbing foil is a quantity which is readily measured. The organisation of a computer calculation to obtain this ratio is discussed. Since the X-ray intensity was in practice measured by a scintillator and photomultiplier, the corrections due to the variation of scintillator efficiency with X-ray energy, which must be incorporated in the calculation, are discussed.

U.K.A.E.A. Research Group,
Culham Laboratory,
Abingdon,
Berks.

January, 1968 (ED)

CONTENTS

		Page
1.	INTRODUCTION	1
2.	THE SPECTRAL DISTRIBUTION OF X-RAY INTENSITY	2
3.	THE VARIATION OF SCINTILLATOR EFFICIENCY WITH X-RAY ENERGY	4
4.	THE ORGANISATION OF THE COMPUTER CALCULATION	8
5.	DISCUSSION OF SOME EXPERIMENTAL RESULTS	12
6.	ACKNOWLEDGEMENT	13
7.	REFERENCES	14
	APPENDIX I X-RAY EMISSION FROM A SOLID BODY IN A PLASMA	15

NOTATION

a – number of different chemical elements in the material of X-ray window

A – constant in equation (10)

$(b-a)$ – number of different chemical elements in the material of the absorber

B – constant in equation (10)

c – velocity of light (cm sec^{-1})

e – electronic charge (e.s.u.)

e_r – error produced in numerical integration

E_A – as defined by equation (1)

E_B – as defined by equation (2)

E_C – as defined by equation (3)

E_D – as defined by equation (4)

E_o – as defined by equation (12)

E_1 – as defined by equation (13)

E_2 – as defined by equation (14)

$F_1(x_1)$ – as defined by Henke, White and Lundberg[9]

$F_2(x_2)$ – as defined by Henke, White and Lundberg[9]

G_1(configuration) – as defined by equation (5)

$G_2(T, n, p_n, q_n)$ – as defined by equation (5)

$G_3(T, \nu)$ – as defined by equation (5)

h – Planck's constant

i – suffix label denoting a particular chemical element

i_p – plasma electron current (e.s.u.)

$I(\nu)$ – absolute spectral intensity for X-rays of frequency ν incident upon the window

$I(\varphi)$ – relative spectral intensity for X-rays of energy φ incident upon the window

$J(U, \nu)$ – X-ray spectral intensity for a frequency ν per steradian per electron incident upon the target with velocity U

k – Boltzmann's constant

m – mass of electron

m_d – mass per square centimetre cross-section of X-ray path of the absorbing element in the scintillator

m_i – mass per square centimetre cross-section in the path of the X-ray beam either of window material or of absorber material for the chemical element labelled i(gm)

$M(u, v, w) \equiv \left(\frac{m}{2\pi kT} \right)^{3/2} \exp \left\{ - \frac{m}{2kT} (u^2 + v^2 + w^2) \right\}$ (Maxwell's velocity distribution)

n – plasma particle density (cm^{-3})

p_n – atomic constants of the plasma atoms

P – K-photon escape probability for a scintillator

q_n – constants associated with X-ray target material

$Q(T)$ – total X-ray energy radiated per square centimetre of solid surface per second per steradian (ergs).

$Q_m(T)$ – measured value of $Q(T)$ on transmission through X-ray window

$r \equiv \frac{\mu_i(\nu_k)}{\mu_i(\nu)}$

$R_1(\nu)$ - attenuation ratio for X-rays of frequency ν in passing through the window

$R_2(\nu)$ - attenuation ratio for X-rays of frequency ν in passing through the absorber

$R_1(\varphi) \equiv R_1\left(\frac{hc}{10^8 e} \cdot \nu\right)$

$R_2(\varphi) \equiv R_2\left(\frac{hc}{10^8 e} \quad \nu\right)$

S - integral $\int_{x_{min}}^{x_{max}} y\, dx$ to be numerically evaluated

T - plasma electron temperature (^oK)

u, v, w - components of electron velocity in Cartesian coordinates

u_s - as defined by equation (1A)

U - velocity of an electron incident upon the X-ray target

$u_r = \sqrt{(u^2 - u_s^2)}$ - component of the electron velocity normal to the sheath after penetration of the sheath (cm sec^{-1})

$u_t = \sqrt{(v^2 + w^2)}$ - component of the electron velocity transverse to the normal to the plasma sheath (cm sec^{-1})

V_s - plasma sheath potential (e.s.u.)

β - probability that a K-electron is involved in a photo-absorption event

ε - angular spherical coordinate in electron velocity space

$\overline{\zeta(\nu)}$ - measured average pulse height for mono-energetic X-rays of frequency ν incident upon a scintillator

$\zeta_p(\nu)$ - measured photopeak pulse height for mono-energetic X-rays of frequency ν incident upon a scintillator

θ - plasma electron temperature in electron volts

$\mu_i(\nu)$ - mass absorption coefficient for an element labelled i at an X-ray frequency ν

$\mu_i(\varphi) \equiv \mu_i\left(\frac{hc}{10^8 e} \cdot \nu\right)$

$\eta(\nu)$ - absolute scintillator efficiency at a frequency ν

$\eta(\varphi) \equiv \frac{\eta(\frac{hc}{10^8 e} \cdot \nu)}{\eta(\frac{hc}{10^8 e} \quad \nu_o)}$ - relative scintillator efficiency for X-rays of energy φ

ν - X-ray frequency (sec^{-1})

ν_o - X-ray frequency at which scintillator is calibrated

ν_k - X-ray frequency for K-radiation (for iodine)

$\xi(U)$ - conversion efficiency for a beam of mono-energetic electrons of velocity U to X-rays. The energy radiated into one steradian in a specific direction being considered

φ - X-ray energy in electron volts

φ_{max} - maximum X-ray energy considered in evaluating X-ray intensity

φ_{min} - minimum X-ray energy considered in evaluating X-ray intensity

φ_{Ki} - X-ray energy for the K-absorption edge of an element labelled i

φ_{Li} - X-ray energy for the L-absorption edge of an element labelled i

ω_k - K-fluorescent yield (for iodine)

1. INTRODUCTION

Consider a beam of X-rays which leaves a plasma through a window, and then passes through an absorbing foil to be detected by a scintillator and photomultiplier. The X-rays may originate either from the volume of the plasma or from a target placed in the plasma.

Let:

ν be the X-ray frequency,

$I(\nu)$ be the spectral distribution of intensity of the X-rays incident upon the window,

$\eta(\nu)$ be the scintillator efficiency at frequency ν.

This efficiency is the fraction of the incident X-ray energy which is converted into light energy. The light energy is measured by the photomultiplier, allowance being made for the fraction of the light produced in the scintillator which reaches the photo-cathode of the photomultiplier. It should be noticed that this is not the true efficiency of the scintillator, which is the ratio of the light energy produced by the scintillator to the X-ray energy absorbed in the scintillator.

Let:

$R_1(\nu)$ be the ratio by which the intensity of X-rays of frequency ν are attenuated on passing through the window,

$R_2(\nu)$ be the ratio by which the intensity of X-rays of frequency ν are attenuated on passing through a further absorber.

Then, ignoring line radiation, the intensity of the X-ray beam incident upon the window is

$$E_A = \int_0^\infty I(\nu)\, d\nu \quad , \qquad \ldots (1)$$

and the intensity as measured by a scintillator is

$$E_B = \int_0^\infty \eta(\nu)\, I(\nu)\, d\nu \quad . \qquad \ldots (2)$$

On passing through the window the X-ray intensity is

$$E_C = \int_0^\infty R_1(\nu)\, \eta(\nu)\, I(\nu)\, d\nu \quad , \qquad \ldots (3)$$

and on further passing through the absorber the intensity is

$$E_D = \int_0^\infty R_2(\nu) \cdot R_1(\nu) \cdot \eta(\nu)\, I(\nu)\, d\nu \quad . \qquad \ldots (4)$$

The window used is transparent to X-rays but not to radiation of lower frequency. That is, there is no contribution to the integral in equation (3) below $\nu = \nu_{min}$, which can be taken as the lower limit in this integral. Further the function $I(\nu)$ is always of a form such that $I(\nu) \to 0$ as $\nu \to \infty$, and there is no contribution to the integral in equation (3) above $\nu = \nu_{max}$, which can be used as the upper limit to this integral.

Let:

n be the plasma particle density (cm^{-3}),

T be the plasma electron temperature (^{o}K),

p_n be atomic constants of the constituent of the plasma,

q_n be constants associated with the material of the target in the plasma.

The function $I(\nu)$ can be written

$$I(\nu) = G_1(\text{configuration}) \cdot G_2(T,n,p_n,q_n) \cdot G_3(T,\nu) \qquad \ldots (5)$$

for the two cases which are to be discussed in the next section. From a brief examination of the problem, it does not seem possible to show that $I(\nu)$ can always be written in this form. Since the integrations in equations (3) and (4) involve $G_3(\ )$ but not $G_1(\ )$ and $G_2(\ )$, the ratio E_D/E_C is a function of T only. Thus, when a measured value of E_D/E_C is compared with a set of calculated values for different electron temperatures, an estimate of the electron temperature is obtained. The discussion of experimental results is postponed to a later section. It should be possible to deduce the plasma density n from absolute measurements of E_C when the functions $G_1(\ )$ and $G_2(\ )$ have been calculated. However it is usually very difficult to obtain a reliable figure.

2. THE SPECTRAL DISTRIBUTION OF X-RAY INTENSITY

(a) Radiation from the volume of the plasma

For the case of a pure hydrogen plasma at a sufficiently high temperature to give X-ray emission the only possible radiation is due to free-free transitions of atomic hydrogen. The function $G_3(T,\nu)$ then approximates to the form $\exp(-h\nu/kT)$. However in practice the radiation due to impurities is often much larger than this free-free radiation. The impurity radiation in general includes free-free, free-bound and line radiation. For free-bound radiation, caused by recombination of a free electron into an excited state of an ion or atom, $G_3(T,\nu) = 0$ for $\nu \leqslant \nu_0$ and $\propto \exp(-h\nu/kT)$ for $\nu > \nu_0$, where $h\nu_0$ is the energy difference between the final bound state and the ionization energy level.

The function $G_2(T,n,p_n)$ refers to the radiation per unit volume of plasma per steradian. For free-free radiation $G_2(T,n,p_n)$ is of the form $n^2/T^{\frac{1}{2}}$ function (p_n). For recombination radiation for an impurity ion of density n_i cm^{-3}, when the ionization potential from the level in question is χ_n, $G_2(T,n,p_n)$ is of the form

$$\frac{n\, n_i}{T^{3/2}} \exp\left(\frac{\chi_n}{kT}\right) \cdot f\,(p_n) .$$

Accurate formulae for $G_2(\ )$ and $G_3(\ )$ are given by Finkelnburg and Peters[1], and details of an experimental determination of T are given by Jahoda et al[2].

(b) Radiation from a target in the plasma

The bombardment of a solid target by electrons gives rise to both line radiation and continuum radiation. The line radiation is characteristic of the material of the solid. The highest frequency line radiation is the characteristic K-radiation of the solid. In our experiments only solids of low atomic number were used. For these solids the frequency of the K-radiation was comparatively low and was completely absorbed in the window.

In general the continuum radiation may originate from a solid target in the plasma, from the walls of the discharge tube or from a thin window set in the wall of the discharge tube. As is shown in Appendix I (equation (A.7), the function $G_3(T,\nu)$ now takes the form

$$\left(\frac{h\nu}{kT} + 2\right) \exp\left(-\frac{h\nu}{kT}\right),$$

and $G_2(T,n,q_n)$ now refers to the energy radiated per square centimetre of target surface per second per steradian. From equations (A.7) and (A.10) in Appendix I and using the equation, $i_I = i_p$, it can be shown that $G_2(\ )$ is of the form $nT^{3/2}\, F(q_n)$. Due to this different form to the function $G_2(\ )$, radiation from the walls becomes more important than volume radiation for plasmas of low density and high temperature.

The formula for $G_2(T,n,q_n) \cdot G_3(T,\nu)$ for radiation from a solid as deduced in Appendix I is almost identical to that used by Aleksin et al[3] in an experiment to determine the electron temperature of a turbulently heated plasma. The deduction of this formula is based upon established work in two fields,

(1) plasma sheaths formed at a boundary of a plasma,

and

(2) the continuum X-ray spectrum produced when mono-energetic electrons bombard a thick target.

3. THE VARIATION OF SCINTILLATOR EFFICIENCY WITH X-RAY ENERGY

The conversion of X-ray energy into light energy which takes place in a scintillator occurs in two steps. The first is the conversion of all or part of the energy in an X-ray photon into the kinetic energy of one or more electrons, and the second is the conversion of the kinetic energy of these electrons into light energy radiated from the scintillator. In the experimental work carried out so far sodium iodide scintillators and plastic scintillators made from the material NE 102A have been used. Previous experimental work[4],[5] suggests that for these two materials the true efficiency of the second process does not vary much with the electron kinetic energy. However, it is known that the true efficiency of the first process does vary with the energy of the incident X-ray photon.

The first correction to be made is to allow for the fraction of the incident X-ray intensity which is not absorbed in passing through the scintillator.

Let:

$\mu_i(\nu)$ be the mass absorption coefficient for the chemical element, labelled i, principally responsible for X-ray absorption in the scintillator,

m_d be the mass per square centimetre cross-section of this chemical element in the path of the X-rays,

$\eta(\nu_o)$ be the scintillator efficiency at some suitably low frequency ν_o at which the scintillator has been calibrated, and at which the incident beam of X-rays is completely absorbed.

N.B. from the remarks in the previous paragraph, provided all the X-ray energy in the incident beam is converted into electron kinetic energy

$$\eta(\nu) = \eta(\nu_o) \ .$$

Then

$$\frac{\eta(\nu)}{\eta(\nu_o)} = 1 - \exp\left\{ -m_d \, \mu_i(\nu) \right\} \qquad \ldots (6)$$

provided $m_d \, \mu_i(\nu_o) \gg 1$. In the case of the plastic scintillator only the X-ray absorption due to carbon was considered, and in the sodium iodide scintillator only the X-ray absorption due to iodine, as the X-ray absorption is due almost entirely to these elements. Ideally the scintillators should always be made sufficiently thick for this correction to be small, but this is not always possible.

For sodium iodide for X-ray energies below 200 keV the predominant absorption process is photo-absorption, in which all the energy of the incident X-ray photon is absorbed[7]. This energy goes into removing an electron from one of the inner shells of the iodine atom

and into kinetic energy acquired by this electron. When the incident X-rays have an energy of less than 33·2 keV it is not possible to remove an electron from the K-shell of the iodine atom, but at greater energies an electron is removed from the K-shell in 84% of the photo-absorption events. In the other 16% of the photo-absorption events an electron is removed from one of the other shells (L,M,N, ...). The probability that the vacancy left in the iodine K-shell gives rise to the emission of an iodine K-photon is known as the fluorescent yield, which for K-photons from iodine is high (87·5%). Further, since the mass absorption coefficient for the fluorescent radiation is comparatively low, the probability that the K-photon escapes from the scintillator can be high.

Write ν_k for the frequency of the K-radiation of iodine. When the K-photon produced escapes from the scintillator the energy deposited in the scintillator is $h\nu - h\nu_k$, otherwise the energy deposited in the scintillator is $h\nu$. When the light output from the scintillator was measured by a photomultiplier, pulses of two different heights were observed, one corresponding to an energy $h\nu$ being deposited in the scintillator, and the other to an energy $h\nu - h\nu_k$. The frequency with which pulses of a given height occurred was measured with a pulse height analyser. Fig.1 shows a plot of the frequency of pulse height against the pulse height obtained from measurement. The probability that the absorption of an incident X-ray photon gives rise to a fluorescent K-photon which escapes from the scintillator is known as the escape probability P. This quantity is equal to the fraction of the total counts under the lower energy peak in Fig.1.

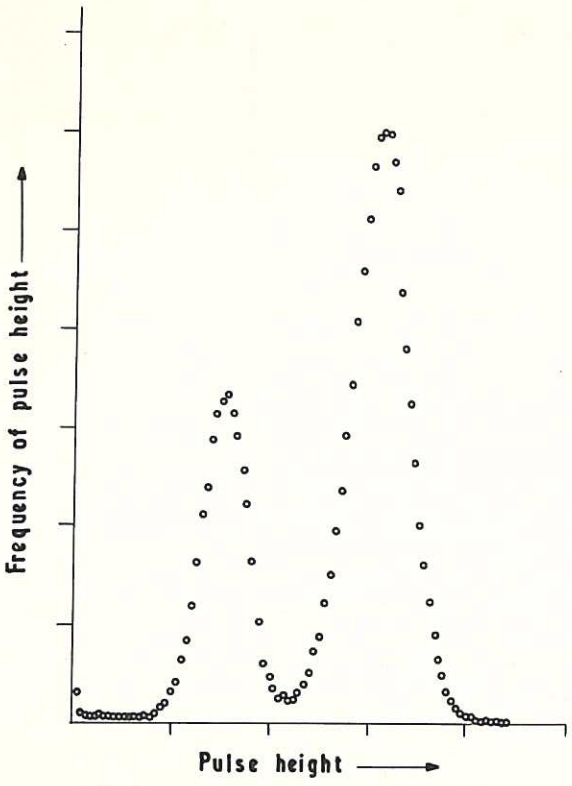

Fig.1 (CLM-R81)
Plot of frequency of pulse height against pulse height for a sodium iodide scintillator.

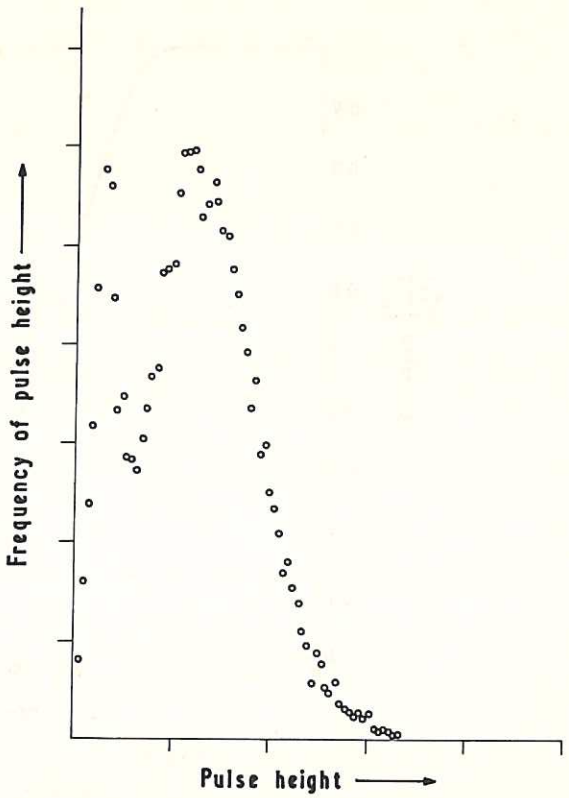

Fig.2 (CLM-R81)
Plot of frequency of pulse height against pulse height for a plastic scintillator (NE102 A) and 35 kV x-rays.

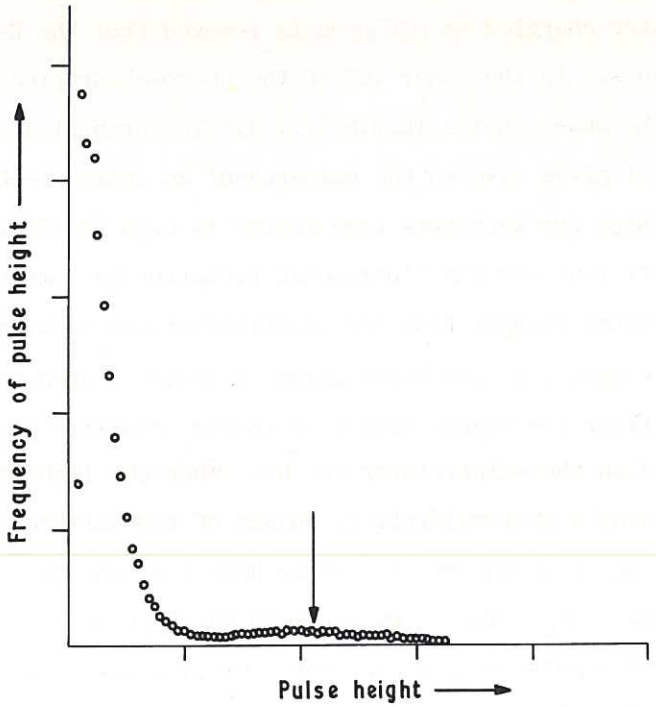

Fig. 3 (CLM-R81)
Plot of frequency of pulse height against pulse height for a plastic scintillator (NE 102 A) and 60 kV γ-rays.

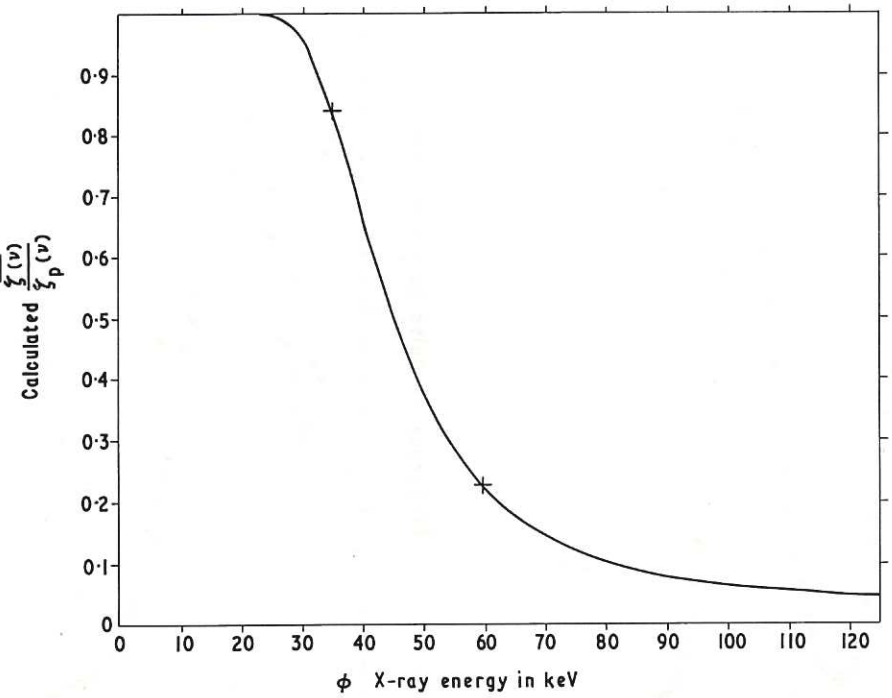

Fig. 4 (CLM-R81)
Plot of the ratio of the mean pulse height to the photopeak pulse height $\zeta(\nu)/\zeta_p(\nu)$ against x-ray energy for a plastic scintillator (NE 102 A).

The escape probability P has been calculated by Axel[6] for the case of a beam of X-rays incident normally on the plane surface of a scintillator which is thick enough to absorb any radiation travelling into the scintillator.

Let: ω_K be the K-fluorescent yield (for iodine 0·875),

β be the probability that a K-electron is involved in a photoabsorption event (for iodine 0·84),

$$r = \frac{\mu_i(\nu_k)}{\mu_i(\nu)} \quad (i \text{ refers to iodine}) .$$

Then the theoretical escape probability is given by[6]

$$P = \frac{\beta\omega_k}{2}\left\{ 1 - r \log_e \left(\frac{r+1}{r}\right) \right\} \qquad \ldots (7)$$

It was experimentally convenient to use a thin sodium iodide crystal on the end of a light-guide. This crystal was too thin for equation (7) to apply. Measurements were made of the escape probability at X-ray energies of 35 keV and 60 keV. An empirical formula was then devised which satisfied these measured values. For a particular scintillator with m_d = 0·075 gm cm^{-2} this formula was $P = 0{\cdot}3130 - 7{\cdot}57 \cdot 10^{-5}\{\mu_i(\nu)\}^2$. From the definition of the escape probability P, it follows that the true scintillator efficiency is given by -{(Probability of K-photon capture X Incident photon energy) + (Probability of K-photon escape X Energy retained)}/Incident photon energy, and hence

$$\frac{\eta(\nu)}{\eta(\nu_o)} = \frac{(1-P)h\nu + P(h\nu - h\nu_k)}{h\nu}\left[1 - \exp\{-m_d\,\mu_i(\nu)\}\right] \qquad \ldots (8)$$

The equation (8) must be used when the energy of the incident X-rays is greater than 33·2 keV; for energies less than this, formula (6) must be used, since the escape probability P is then zero.

For the plastic scintillator NE102A X-ray absorption is due to both photo-electric absorption and Compton scattering. Photo-electric absorption varies approximately as $1/\nu^3$, but Compton scattering varies slowly with frequency[7]. Thus at higher X-ray frequencies the effect of Compton scattering is dominant. For a plastic scintillator, where the X-ray absorption is due to carbon, the two effects are comparable for an X-ray energy of 20 keV, whereas for sodium iodide the two effects are comparable for an X-ray energy of 200 keV. For the measurements considered it was necessary to take account of the effects of Compton scattering in plastic scintillators, but not for sodium iodide scintillators.

Fig.2 is a plot of the frequency of pulses against pulse height obtained from pulse height analyser measurements. The scintillator used was NE102A 3·81 cm dia ×2·54 cm long and the X-rays incident upon the scintillator were fluorescent X-rays from ceric oxide (35 keV). The high energy peak corresponds to events where all the energy of the incident X-ray photon is absorbed and is known as the photopeak. The lower energy peak corresponds to Compton scattering where only a part of the energy of the incident photon is absorbed. Fig.3 shows a similar plot under similar conditions, but with γ-rays (60 keV) from americium 241 incident upon the scintillator. The effect of Compton scattering is now dominant

and the position of the much attenuated photo-peak is indicated by the arrow. The pulse heights corresponding to the photo-peaks shown in Figs.2 and 3 are proportional to the energy of the incident X-ray photons as they should be. However the effective scintillation efficiency is proportional to the average pulse height obtained from the graphs in Figs.2 and 3.

Let:

$\overline{\zeta(\nu)}$ be the average pulse height,

$\zeta_p(\nu)$ be the pulse height of the photo-peak.

The scintillator efficiency is now given by

$$\frac{\eta(\nu)}{\eta(\nu_o)} = \frac{\overline{\zeta(\nu)}}{\zeta_p(\nu)} \left[1 - \exp \left\{ -m_d \underset{\text{carbon}}{\mu} (\nu) \right\} \right] \qquad \ldots (9)$$

It was assumed that the variation of $\overline{\zeta(\nu)}/\zeta_p(\nu)$ could be expressed by an empirical formula

$$\frac{\overline{\zeta(\nu)}}{\zeta_p(\nu)} = 1 - \exp \left\{ - \frac{A}{\nu^{\frac{1}{2}}} - \frac{B}{\nu^4} \right\} \qquad \ldots (10)$$

Fig.4 shows the result of adjusting the values of A and B in equation (10) so that the measured values of $\overline{\zeta(\nu)}/\zeta_p(\nu)$ corresponding to Figs.2 and 3, shown as crosses, fit the curve. Fig.4 shows that the scintillator efficiency does not fall until well above the X-ray energy at which the effects of photo-absorption and Compton scattering are comparable (20 keV). A similar result has been obtained by Berger and Doggett[8] for sodium iodide scintillators. This is due to the fact that at higher X-ray energies most of the pulses under the photopeak correspond to events in which the Compton scattering of an incident X-ray photon is followed by photo-absorption.

4. THE ORGANISATION OF THE COMPUTER CALCULATION

It is convenient to write φ for the X-ray energy in electron volts and θ for the electron temperature also in electron volts.

There are now the relations

$$\left.\begin{aligned} \nu &= \varphi \cdot \frac{10^8 e}{hc} \\ T &= \theta \cdot \frac{10^8 e}{kc} \\ \frac{h\nu}{kT} &= \frac{\varphi}{\theta} \\ d\nu &= \frac{10^8 e}{hc} d\varphi \end{aligned}\right\} \qquad \ldots (11)$$

This calculation is not concerned with the absolute value of X-ray intensity, and since only integration over X-ray frequency is concerned the functions $G_1(\ )$ and $G_2(\ )$ will be ignored. The function $I(\varphi)$ was normalised so that

$$E_o = \int_o^\infty I(\varphi)\, d\varphi = 1 \qquad \ldots (12)$$

Then for radiation from the volume of the plasma

$$I(\varphi) = \frac{1}{\theta} \exp\left(-\frac{\varphi}{\theta}\right) ,$$

and for radiation from a solid target

$$I(\varphi) = \frac{1}{3\theta}\left(\frac{\varphi}{\theta} + 2\right) \exp\left(-\frac{\varphi}{\theta}\right) .$$

When the scintillator efficiency is written as a function of the variable φ write

$$\frac{\eta(\nu)}{\eta(\nu_o)} = \eta(\varphi)$$

where $\eta(\nu_o)$ is the scintillator efficiency at a low X-ray frequency ν_o, so that as $\varphi \to 0$, $\eta(\varphi) \to 1$. $R_1(\varphi)$ and $R_2(\varphi)$ are identically equal to $R_1\left(\frac{hc}{10^8 e} \cdot \nu\right)$ and $R_2\left(\frac{hc}{10^8 e} \cdot \nu\right)$ respectively. In place of the limits 0 and ∞ in equation (3) limits φ_{min} and φ_{max} are taken. Below φ_{min}, $R_1(\varphi)$ becomes very small, and above φ_{max}, $I(\varphi)$ becomes very small. Equation (3) now takes the form

$$E_1 = \int_{\varphi_{min}}^{\varphi_{max}} R_1(\varphi)\ \eta(\varphi)\ I(\varphi)\, d\varphi \qquad \ldots (13)$$

and similarly equation (4) becomes

$$E_2 = \int_{\varphi_{min}}^{\varphi_{max}} R_1(\varphi) \cdot R_2(\varphi) \cdot \eta(\varphi) \cdot I(\varphi)\, d\varphi \qquad \ldots (14)$$

Now

$$E_2/E_1 = E_D/E_C$$

The way in which the quantity $R_1(\varphi)\ \eta(\varphi)\ I(\varphi)$ varied with φ made it difficult to use a standard numerical integration technique. The numerical integration was easier after the transformation, $\psi = \log_e\left(\frac{\varphi}{\theta}\right)$, had been made. Equation (12) then becomes

$$E_1 = \int_{\psi_{min}}^{\psi_{max}} R_1\{\theta \exp(\psi)\}\ \eta\{\theta \exp(\psi)\}\ I\{\theta \exp(\psi)\}\ \theta \exp(\psi)\, d\psi \qquad \ldots (15)$$

where $\psi_{max} = \log_e\left(\frac{\varphi_{max}}{\theta}\right)$, $\psi_{min} = \log_e\left(\frac{\varphi_{min}}{\theta}\right)$.

The material of the window contains a number 'a' of different chemical elements whose mass absorption coefficients for X-rays are μ_i, and the mass per square centimetre cross-section in the path of the X-rays is m_i for the element labelled 'i'. The function $R_1(\varphi)$ is given by

$$R_1(\varphi) = \exp\left[-\sum_{i=1}^{i=a}\{m_i\,\mu_i(\varphi)\}\right] \qquad \ldots (16)$$

The absorber consists of a number of chemical elements (b - a) and $R_2(\varphi)$ is given by

$$R_2(\varphi) = \exp\left[-\sum_{i=a+1}^{i=b}\{m_i\,\mu_i(\varphi)\}\right]$$

$$\therefore\ R_1(\varphi)\cdot R_2(\varphi) = \exp\left[-\sum_{i=1}^{i=a}\{m_i\,\mu_i(\varphi)\}\right]\cdot\exp\left[-\sum_{i=a+1}^{i=b}\{m_i\,\mu_i(\varphi)\}\right]$$

$$= \exp\left[-\sum_{i=1}^{i=b}\{m_i\,\mu_i(\varphi)\}\right] \qquad \ldots (17)$$

Over considerable ranges of φ the functions $\mu_i(\varphi)$ approximate to the form const/φ^3. However, at certain values of φ, φ_{ki} and φ_{Li} characteristic of a given chemical element, the value of $\mu_i(\varphi)$ increases very sharply with increasing φ. In this calculation these sharp increases have been approximated by mathematical discontinuities, different formulae being used for $\varphi > \varphi_{ki}$ and $\varphi < \varphi_{ki}$. For $\varphi > 3000$ eV $\mu_i(\varphi)$ was calculated mostly from the empirical formulae of Victoreen[7], and for $\varphi < 3000$ eV $\mu_i(\varphi)$ was calculated mostly from the empirical formulae of Henke, White and Lundberg[9]. Both of these sets of formulae are based upon previously determined experimental values. The value of φ at the discontinuity $\varphi = \varphi_{Li}$ was small and the corresponding value of $\mu_i(\varphi)$ large. For $\varphi < \varphi_{Li}$, $\mu_i(\varphi)$ was taken as constant at the value of φ slightly greater than φ_{Li}. In nearly all cases of practical interest this does not much affect the calculation as $R_1(\varphi)$ and $R_1(\varphi)\cdot R_2(\varphi)$ as given by equations (15) and (16) are then very small. For iodine when $\varphi_{Li} < \varphi < \varphi_{Ki}$ an empirical formula for the mass absorption coefficient $\mu_i(\varphi)$ was devised to fit previously measured values of this quantity. This formula was

$$\mu_i(\varphi) = \frac{97{\cdot}68}{\varphi}\,F_2\left\{\frac{3622}{\varphi} + \frac{9{\cdot}232.10^6}{\varphi^2}\right\},$$

where the function $F_2(\ )$ was as defined by Henke, White and Lundberg[9].

The computer integration was performed by a subroutine QAO2A, now in the Culham computer library. This subroutine evaluates an integral

$$S = \int_{x_{min}}^{x_{max}} y \, dx \qquad \ldots (18)$$

using Simpson's rule. Consider five successive ordinates y_{n-2}, y_{n-1}, y_n, y_{n+1}, y_{n+2} corresponding to five successive abscissae x_{n-2}, x_{n-1}, x_n, x_{n+1}, x_{n+2}, where $x_{n-2} = x_n - 2\Delta x$, $x_{n-1} = x_n - \Delta x$, $x_{n+1} = x_n + \Delta x$, $x_{n+2} = x_n + 2\Delta x$. The error e_r produced by using Simpson's rule to evaluate this part of the integral is given by

$$e_r = \frac{x_{n+2} - x_{n-2}}{180} \left\{ y_{n-2} - 4y_{n-1} + 6y_n - 4y_{n+1} + y_{n+2} \right\} .$$

The subroutine measures this error and continuously adjusts the step length Δx so that the error is kept within a prescribed limit.

Due to this method of evaluating the integral, it is not possible to use the subroutine over a range of φ in which one of the discontinuities in $\mu_i(\varphi)$ occurs. In evaluating the integrals E_1 and E_2 it was necessary to split the range of integration as follows: (φ_{min} to $\varphi_{Q1} - \Delta\varphi$), ($\varphi_{Q1} + \Delta\varphi$ to $\varphi_{Q2} - \Delta\varphi$) ... ($\varphi_{QN} + \Delta\varphi$ to φ_{max}), where the values φ_{Q1}, φ_{Q2} ... φ_{QN} are the discontinuities appropriate to a particular calculation. The selection of the appropriate values of φ_{Ki} and the successive calling of the subroutine QAO2A for the integration over these intervals was done in the MAIN programme. Computer function subprogrammes and subroutines were used to calculate the quantities required as follows:-

Computer function subprogramme or subroutine	Expression as formulated in this report
AMU(MA, PHI)	$\mu_i(\varphi)$
F1(ARG)	$F_1(x_1)$ } Henke, White and
F2(ARG)	$F_2(x_2)$ } Lundberg[9]
F3(ARG)	$\sigma_o \pi \ell_o^2 N_o$ (Victoreen[7])
R1(IW, WM, PHI)	$-m_d \, \mu_i(\varphi)$
R2(NA, PM, PHI, INDIC)	$-\sum_{i=1}^{i=a} m_i \, \mu_i(\varphi)$
INTEG1 (PHI, Y)	$R_1\{\theta\exp(\psi)\}\eta\{\theta\exp(\psi)\}I\{\theta\exp(\psi)\}\theta\exp(\psi)$
INTEG2(PHI, Y)	$R_1\{\theta\exp(\psi)\}R_2\{\theta\exp(\psi)\}\eta\{\theta\exp(\psi)\}I\{\theta\exp(\psi)\}\theta\exp(\psi)$.

A prelude was used, and the common variables were, in the notation of this report, a, b, i, m_i, m_d i (for the scintillator material) and θ. The common variables were only used in the MAIN programme and in the subroutines INTEG1(PHI, Y) and INTEG2(PHI, Y).

The subroutine QA02A was adjusted to give an accuracy of about 1 part in 10^4. The accuracy of $\mu_i(\varphi)$, given by the empirical formulae mentioned (references (7) and (9)) is however, only claimed to be 1 part in 100, and this clearly sets a limit on the accuracy of the evaluation of E_1 and E_2.

5. DISCUSSION OF SOME EXPERIMENTAL RESULTS

X-ray absorption measurements have been used to estimate the electron temperature of a turbulently heated plasma in the 'Twist' experiment. The higher plasma densities gave rise to electron temperatures of the order of 2000 eV. The measurements were then made with a graphite target in the plasma and a thin (0·0005 in.) beryllium window. Lower plasma densities gave rise to a higher electron temperature of about 20000 eV. In this case X-rays originating from the torus wall were measured after passing through the torus wall and also through a surrounding copper sheath.

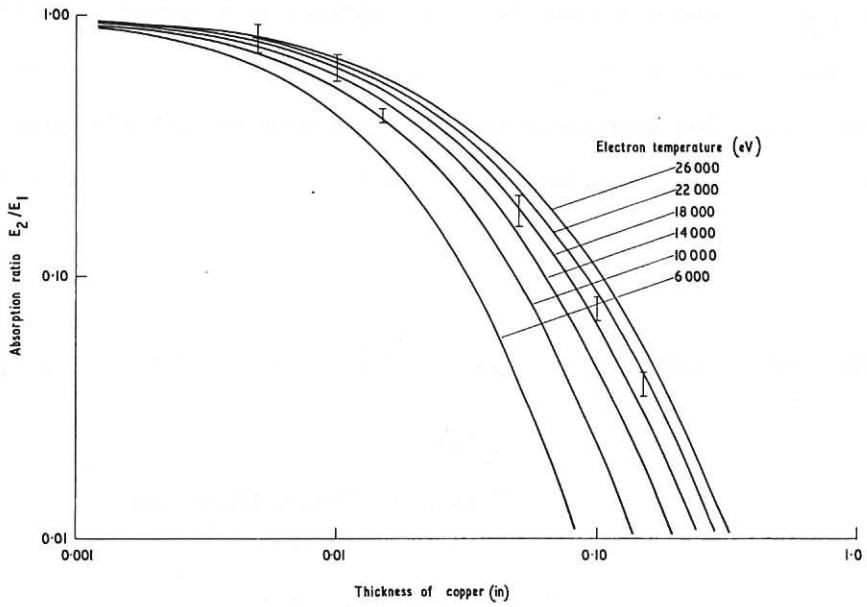

Fig. 5 (CLM-R81)
Plot of calculated values of E_2/E_1 against thickness of absorber, and corresponding measured values (shown as error bars).

Measured and calculated quantities for this latter case are shown in Fig.5. Here calculated values of E_2/E_1 are plotted against the thickness of absorber for different assumed electron temperatures. Experimentally determined values for the conditions calculated are inserted as error bars. It is clear from this figure that the experimental values are consistent with an electron temperature of about 20000 eV. Fig.6 shows

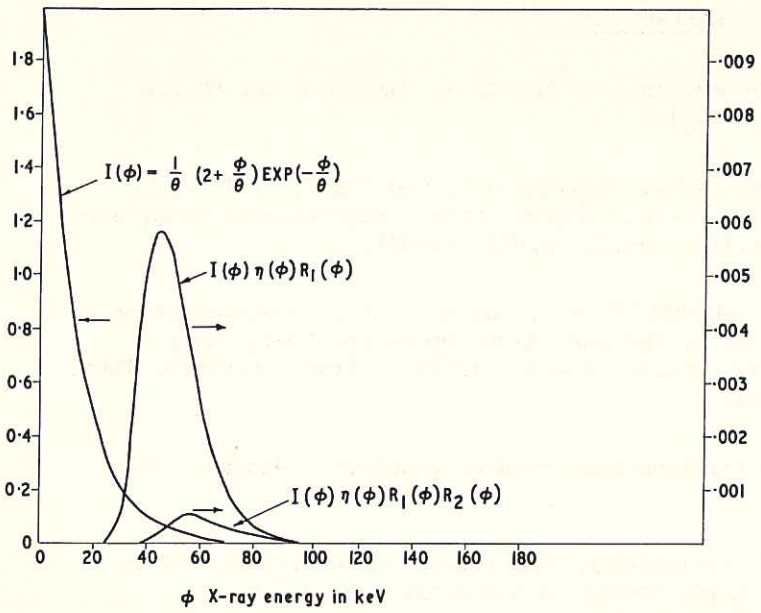

Fig.6 (CLM-R81)
Plot of spectral intensities of continuum radiation: $I(\phi)$ in the plasma, $I(\phi)\,n(\phi)\,R_1(\phi)$ on passing through window $I(\phi)\,n(\phi).R_1(\phi)\,R_2(\phi)$ on further passing through absorber.

plots of the theoretical quantities $I(\varphi)$, $I(\varphi) \cdot \eta(\varphi) \cdot R_1(\varphi)$ and $I(\varphi) \cdot \eta(\varphi) \cdot R_1(\varphi) \cdot R_2(\varphi)$ for the conditions as in Fig.5 but with an assumed electron temperature of 10000 eV.

Fig.5 indicates the general correctness of the entire calculation, but in comparing theory with experiment a reasonable estimate (within 20-30%) of the plasma electron temperature is only obtained for the thicker absorbers (> ·03 in.).

6. ACKNOWLEDGEMENT

The authors are indebted to Dr S.M. Hamberger and Mr R.B. Owen of A.E.R.E. Harwell for helpful discussion of this work.

7. REFERENCES

1. FINKELNBURG, W. and PETERS, T. Kontinuierliche Spektren. Handbuch der Physik (S. Flugge, Ed.), vol.28, p.79 (1957).

2. JAHODA, F.C., LITTLE, E.M., QUINN, W.E., SAWYER, G.A. and STRATTON, T.F. Continuum radiation in the X-ray and visible regions from a magnetically compressed plasma (Scylla). Phys. Rev., vol.119, no.3, p.843 (1960).

3. ALEKSIN, V.F., SUPRUNENKO, V.A., SUKHOMLIN, E.A. and REVA, N.I. Determination of the electron temperature of a plasma by the soft X-ray bremsstrahlung. Soviet Physics - Technical Physics vol.11, no.4, p.465 (1966). (Trans. from Zh. Tekh. Fiz. vol.36, no.4, p.620 (1966).

4. MOTT, W.E. and SUTTON, R.B. Scintillation and Cerenkov counters. Handbuch der Physik, vol.45, p.86 (1958).

5. ADLAM, J.H. and BURCHAM, J.N. The variation of the conversion efficiency of an NE102A plastic scintillator with X-ray energy in the range 1·8 - 4·5 keV. J. Sci. Instr., vol.43, p.93 (1966).

6. AXEL, P. Intensity corrections for iodine X-rays escaping from sodium iodide scintillation crystals. Rev. Sci. Instr., vol.25, p.391 (1954).

7. VICTOREEN, J.A. The calculation of X-ray mass absorption coefficients. J. Appl. Phys., vol.20, p.1141 (1949).

8. BERGER, M.J. and DOGGETT, J. Response function of NaI(Tℓ) scintillation counters. Rev. Sci. Instr., vol.27, p.269 (1956).

9. HENKE, B.L., WHITE, R. and LUNDBERG, B. Semiempirical determination of mass absorption coefficients for the 5 to 50 Angstrom X-ray region. J. Appl. Phys., vol.28, p.98 (1957).

10. DYSON, N.A. The continuous X-ray spectrum from electron-opaque targets. Proc. Phys. Soc., vol.73, p.924 (1959).

11. ALLEN, J.E., BOYD, R.L.F., REYNOLDS, P. The collection of positive ions by a probe immersed in a plasma. Proc. Phys. Soc. B, vol.70, p.297 (1957).

APPENDIX I

X-RAY EMISSION FROM A SOLID BODY IN A PLASMA

Let there be a solid body in the plane x = 0 of a Cartesian coordinate system, and a plasma sheath such that only electrons with a velocity component in the x-direction greater than u_s can penetrate the sheath, where u_s is given by the expression

$$\tfrac{1}{2} m u_s^2 = e V_s \qquad \ldots (A.1)$$

$-V_s$ being the sheath potential.

Assuming the density in velocity space is given by

$$n M(u, v, w)\, du\, dv\, dw = n \left(\frac{m}{2\pi kT} \right)^{3/2} \exp \left\{ - \frac{m}{2kT}(u^2 + v^2 + w^2) \right\} \cdot du\, dv\, dw$$

Then the number of electrons penetrating the plasma sheath per cm^2 per sec

$$= \frac{i_p}{e}$$

$$= n \int_{u_s}^{\infty} M(u, v, w)\, u\, du\, dv\, dw \qquad \ldots (A.2)$$

and integrating

$$= n \left(\frac{kT}{2\pi m} \right)^{1/2} \exp \left(- \frac{mu_s^2}{kT} \right) \qquad \ldots (A.3)$$

It has been shown experimentally by Dyson[10] that the X-ray spectral intensity produced per electron with velocity U incident upon the target, is of the form

$$\begin{cases} E(U, \nu) = A_1 \left(\frac{mU^2}{2h} - \nu \right) d\nu & , \quad \nu < \frac{mU^2}{2h} \\ = 0 & , \quad \nu > \frac{mU^2}{2h} \end{cases} \qquad \ldots (A.4)$$

Write

$$F(U) = \int_0^{\infty} E(U, \nu)\, d\nu$$

Substituting from equation (A.4)

$$= \frac{A_1}{2} \left(\frac{mU^2}{2h} \right)^2$$

The X-ray conversion efficiency ξ

$$= \frac{F(U)}{\frac{1}{2}mU^2} = A_1 \frac{mU^2}{4h^2}$$

$$\therefore \quad A_1 = \frac{4h^2 \xi}{mU^2}$$

The X-ray conversion efficiency ξ, as measured in an X-ray tube, is usually given for a certain electron energy φ_1 eV. Then

$$\tfrac{1}{2}\, mU^2 = e\varphi_1/300 \qquad \ldots (A.5)$$

$$\therefore \quad A_1 = \frac{2h^2\, \xi \cdot 300}{e\varphi_1}$$

The quantity ξ and hence A_1 refers to the energy emitted per second per steradian in a given direction. Then the spectral intensity of X-rays again referring to energy emitted per steradian per second in a given direction is given by

$$I(\nu) = 2\pi A_1 n \iint_{u_r^2+u_t^2=\frac{2h\nu}{m}}^{\infty} \left\{ \frac{m(u_r^2+u_t^2)}{2h} - \nu \right\} \left(\frac{m}{2\pi kT}\right)^{3/2} \exp\left(-\frac{mu_s^2}{2kT}\right) \times \exp\left\{-\frac{m}{2kT}(u_r^2+u_t^2)\right\} u_r\, u_t\, du_r\, du_r$$

Write

$$u_r = u_q \cos \cdot \varepsilon$$

$$u_t = u_q \sin \cdot \varepsilon$$

$$\therefore \quad \frac{\partial(u_r,\, u_t)}{\partial(u_q,\, \varepsilon)} = u_q$$

Transforming the integration variable

$$I(\nu) = 2\pi A_1 n \left(\frac{m}{2\pi kT}\right)^{3/2} \exp\left(-\frac{mu_s^2}{2kT}\right) \int_{\varepsilon=0}^{\varepsilon=\frac{\pi}{2}} \int_{u_q=\sqrt{(\frac{2h\nu}{m})}}^{\infty} \left(\frac{mu_q^2}{2h} - \nu\right) \exp\left(-\frac{mu_q^2}{2kT}\right) \times u_q^3 \cos.\varepsilon \cdot \sin.\varepsilon \cdot d\varepsilon \cdot du_q$$

$$\ldots (A.6)$$

$$= 2\pi A_1 n \left(\frac{m}{2\pi kT}\right)^{3/2} \exp\left(-\frac{mu_s^2}{2kT}\right) \int_{u_q=\sqrt{(\frac{2h\nu}{m})}}^{\infty} \left(\frac{mu_q^2}{2h} - \nu\right) \exp\left(-\frac{mu_q^2}{2kT}\right) u_q^3 du_q \times \int_{\varepsilon=0}^{\varepsilon=\frac{\pi}{2}} \cos\varepsilon \sin\varepsilon\, d\varepsilon$$

Integrating equation (A.6) becomes

$$I(\nu) = \frac{A_1 n}{\sqrt{(2\pi)}} \left(\frac{kT}{m}\right)^{3/2} \frac{m}{h} \exp\left(-\frac{mu_s^2}{2kT}\right) \left(\frac{h\nu}{kT} + 2\right) \exp\left(-\frac{h\nu}{kT}\right)$$

Substituting from equations (A.3) and (A.5)

$$I(\nu) = i_p \frac{2h\xi kT300}{\sqrt{(2\pi)}e2\varphi_1} \left(\frac{h\nu}{kT} + 2\right) \exp\left(-\frac{h\nu}{kT}\right) \qquad \ldots (A.7)$$

Write

$$Q(T) = \int_0^{\infty} I(\nu)\, d\nu$$

Then from equation (11) and (12)

$$Q(T) = i_p \cdot \frac{2h\xi kT\ 300}{\sqrt{(2\pi)}e^2\varphi_1} E_o \cdot \frac{kT}{h}$$

and since for this case $E_o = 1$

$$Q(T) = i_p \cdot \frac{2\xi k^2T^2\ 300}{\sqrt{(2\pi)} \cdot e^2\varphi_1} \qquad \ldots (A.8)$$

Write $Q_m(T)$ for the measured value of $Q(T)$ on transmission through the X-ray window, allowing for the variation of the scintillator efficiency with X-ray frequency. Then from equations (11) and (13)

$$Q_m(T) = i_p \frac{2\xi k^2T^2\ 300}{\sqrt{(2\pi)} \cdot e^2\varphi_1} \cdot \frac{E_1}{\eta(\nu_o)} \qquad \ldots (A.9)$$

For the case of an insulated target in a plasma the net current from the target is zero, and the ion current to the target is equal to the electron current. Allen, Boyd and Reynolds[11] give the formula for the ion current i_I as

$$i_I = n\ e\ A_2 \left(\frac{kT}{M}\right)^{\frac{1}{2}} \qquad \ldots (A.10)$$

where M is the ion mass and A_2 is a constant whose value is uncertain, but

$$1 < A_2 < 1{\cdot}227$$

Equating $i_I = i_P$ and substituting the value of i_I given by equation (A.10) into equation (A.9)

$$Q_m(T) = \frac{2A_2\xi\ 300}{\sqrt{(2\pi)} \cdot e^2\varphi_1\ \eta(\nu_o)} \cdot n\ (kT)^{\frac{5}{2}} E_1 \ . \qquad \ldots (A.11)$$

Available from

HER MAJESTY'S STATIONERY OFFICE

49 High Holborn, London, W.C.1
423 Oxford Street, London W.1
13a Castle Street, Edinburgh 2
109 St. Mary Street, Cardiff CF1 1JW
Brazennose Street, Manchester 2
50 Fairfax Street, Bristol 1
258-259 Broad Street, Birmingham 1
7-11 Linenhall Street, Belfast BT2 8AY

or through any bookseller.

Printed in England

S.O. Code No. 91-3-21-92